JOURNAL OF TISSUE ENGINEERING AND REGENERATIVE MEDICINE
J Tissue Eng Regen Med 2018; **12**: e579–e591.
Published online 22 March 2017 in Wiley Online Library (wileyonlinelibrary.com) **DOI:** 10.1002/term.2330

RESEARCH ARTICLE

Human umbilical cord derivatives regenerate intervertebral disc

Naimisha Beeravolu[1,2], Jared Brougham[3], Irfan Khan[1,2,4], Christina McKee[1,2], Mick Perez-Cruet[2,5] and G. Rasul Chaudhry[1,2]*

[1]*Department of Biological Sciences, Oakland University, Rochester, Michigan, USA*
[2]*OUWB Institute for Stem Cell and Regenerative Medicine, Rochester, Michigan, USA*
[3]*OUWB School of Medicine, Oakland University, Rochester, Michigan, USA*
[4]*Dr Panjwani Center for Molecular Medicine and Drug Research, International Center for Chemical and Biological Sciences, University of Karachi, Karachi, Pakistan*
[5]*Beaumont Health System, Royal Oak, Michigan, USA*

Abstract

Intervertebral disc (IVD) degeneration is characterized by the loss of nucleus pulposus (NP), which is a common cause for lower back pain. Although, currently, there is no cure for the degenerative disc disease, stem cell therapy is increasingly being considered for its treatment. In this study, we investigated the feasibility and efficacy of human umbilical cord mesenchymal stem cells (MSCs) and chondroprogenitor cells (CPCs) derived from those cells to regenerate damaged IVD in a rabbit model. Transplanted cells survived, engrafted and dispersed into NP *in situ*. Significant improvement in the histology, cellularity, extracellular matrix proteins, and water and glycosaminoglycan contents in IVD recipients of CPCs was observed compared to MSCs. In addition, IVDs receiving CPCs exhibited higher expression of NP-specific human markers, SOX9, aggrecan, collagen 2, FOXF1 and KRT19. The novelty of the study is that *in vitro* differentiated CPCs derived from umbilical cord MSCs, demonstrated far greater capacity to regenerate damaged IVDs, which provides basis and impetus for stem cell based clinical studies to treat degenerative disc disease. Copyright © 2016 John Wiley & Sons, Ltd.

Received 22 March 2016; Revised 3 August 2016; Accepted 26 September 2016

Keywords **Tissue engineering; Cell therapy; Intervertebral disc; Human umbilical cord mesenchymal stem cells; Chondroprogenitor cells; Rabbit model; Glycosaminoglycan**

1. Introduction

Lower back pain is one of the most common disabilities in approximately 80% of the adult population, leading to significant discomfort, emotional distress, and socioeconomic burden (Pfleger, 2003). Degeneration of the intervertebral disc (IVD) is one of the leading causes for lower back pain. The IVD is an avascular, aneural tissue with low cell density, composed of the annular fibrosus (AF), nucleus pulposus (NP) and the end plates (Clouet *et al*., 2011). A healthy disc consists of about 1% of NP tissue by volume, which is predominantly comprised of extracellular matrix (ECM) that is rich in proteoglycans and sulfated glycosaminoglycans (sGAG). The NP allows the retention of water content in the disc and provides shock absorption and maintains IVD homeostasis (Ciapetti *et al*., 2012). In humans, the NP transitions from highly vacuolated notochordal tissue into a fibrocartilaginous tissue by the second decade of life (Kim *et al.*, 2003). The loss of NP results in reduction of water, sGAG contents and ECM proteins leading to degenerative disc disease (DDD). Currently, there is no cure to restore the physiological and anatomical functionalities of the degenerated IVD. Spinal fusion is often practiced to mitigate pain resulting from DDD. Alternatively, allografts and metal implants are used with modest success as their availability and compatibility are very limited (Amini *et al.*, 2012; Nouh, 2012).

Recently, stem cell-based therapies have been increasingly considered for treating degenerative diseases including DDD. Embryonic stem cells (ESCs) have the greatest therapeutic potential and in one of our earlier studies we have shown that chondrogenic derivatives of ESCs transplanted into a rabbit model of DDD survived, integrated and produced ECM (Sheikh *et al*., 2009). However, the isolation of ESCs involves destruction or manipulation of the preimplantation stage embryo. Therefore, ethical and moral concerns have hindered further development of ESCs based therapies (Espinoza and Peterson, 2012; Lo and Parham, 2009; Pera, 2001).

Mesenchymal stem cells (MSCs) derived from adult tissues such as bone marrow (BM) and adipose MSCs have also been studied for their potential to differentiate into chondrogenic or NP-like cells capable of producing extracellular matrix *in vitro*. MSCs were reported to be induced by various growth factors such as transforming growth factor (TGF)β, insulin-like growth factor 1 and growth differentiation factor (GDF)6 to express NP-specific markers

*Correspondence to: G. Rasul Chaudhry, Department of Biological Sciences, Oakland University, Rochester, Michigan, 48309 USA. E-mail: chaudhry@oakland.edu

(Bian and Sun, 2015; Clarke *et al*., 2014; Colombier *et al*., 2016; Gupta *et al*., 2011), while coculturing with BM-MSCs with NP cells resulted in differentiation into cells that express NP-specific markers including aggrecan (ACAN), Versican, Sox9, Col2 and Col6 (Shim *et al*., 2016; Strassburg *et al*., 2010). Similarly, differentiation of human BM-MSCs into NP phenotypes was achieved by porcine notochordal cells (Korecki *et al*., 2010; Purmessur *et al*., 2011). Adipose stem cells cocultured with human NP cells stimulated matrix synthesis and cell proliferation of NP cells (Song *et al*., 2015). Adult stem cells have also been tested to regenerate IVD using animal models (Chun *et al*., 2012; Henriksson *et al*., 2009; Jeong *et al*., 2010; Marfia *et al*., 2014). However, isolation of MSCs from adult sources is invasive and the cells have shown limited proliferation and differentiation potential. Furthermore, adult MSCs might have undergone genetic changes due to aging and exposure to environmental pollutants (Bentivegna *et al*., 2013; Liu *et al*., 2013; Teschendorff *et al*., 2012). In contrast, isolation of MSCs from perinatal sources such as umbilical cord (UC) blood, cord tissue, and placenta is noninvasive. Also, they are more primitive and display a lower risk of graft-vs.-host disease as compared to BM-MSCs (Arufe *et al*., 2011; Hua *et al*., 2011). In one of the studies, Wharton's jelly-derived MSCs were induced to differentiate into chondrogenic lineage by culturing on laminin coated plates. The differentiated cells shared features with immature NP cells, and produced sGAG and matrix proteins (Chon *et al*., 2013). Another study reported differentiation of CB MSCs into chondrocyte-like cells when cultured in rabbit IVD explants and produced proteoglycan rich extracellular matrix (ECM) (Anderson *et al*., 2013). Like adult stem cells, perinatal stem cells have been investigated for their potential to regenerate IVD using animal models. UC-derived cells improved histological and biomechanical properties of the degenerated IVD when injected into the NP region of rabbit IVDs (Leckie *et al*., 2013). Recently, Wharton's jelly MSCs transplanted into damaged IVDs of animal models have reported improvement in the disc water content and histology (Ahn *et al*., 2015) and upregulation of genes and proteins involved in disc matrix formation (Zhang *et al*., 2015). In a clinical study, UC cells transplanted to the IVDs of two individuals with chronic discogenic low back pain appeared to facilitate alleviation of pain and improvement in the physical function, but showed no change in the magnetic resonance imaging (MRI) signal intensity of the disc (Pang *et al*., 2014). Not only was this study conducted on a limited number of patients, but the transplanted cells were not well characterized. It is imperative that clinical trials should proceed with well-planned studies and thorough analysis of characteristics and potential to produce components of ECM both *in vitro* and *in vivo*. We hypothesize that predifferentiation of the MSCs into chondroprogenitor cells (CPCs) would be more effective in producing ECM and regenerating NP of the IVD. To our knowledge, this is the first report to compare the therapeutic potential of UC-MSCs and CPCs to regenerate NP in an animal model. The results demonstrated that CPCs were more efficacious. These findings are expected to provide further impetus and basis for developing strategies to treat human DDD using UC-MSCs and their derivatives.

2. Materials and methods

2.1. Isolation, characterization, and cultivation of human umbilical cord mesenchymal stem cells

Human UC samples were obtained from consented healthy donors through the Beaumont Hospital BioBank and isolation of MSCs was carried out at Oakland University under approved protocols (HIC# 2012-101 and IRB# 400244, respectively). UC-MSCs were isolated and characterized in our laboratory (Alghamdi *et al*., 2016; Beeravolu *et al*., 2016). Briefly, the UC samples were rinsed in phosphate-buffered saline (PBS) to remove blood clots and then minced into approximately 1–2 mm pieces. The tissue pieces were plated in 75 cm^2 culture flasks for explant culture using growth medium containing high-glucose Dulbecco's modified Eagle's medium (DMEM; Life Technologies, Carlsbad, CA, USA), supplemented with 10% fetal bovine serum (FBS; Aleken Biologicals, Nash, TX, USA), and 5.6% of antibiotic solution (0.1% gentamicin, 0.2% streptomycin, and 0.12% penicillin; Sigma, St Louis, MO, USA) and incubated at 37°C in an atmosphere of 5% CO_2 in a humidified incubator. Out growth cells from explants were passaged upon reaching 70–80% confluency and characterized using fluorescence-activated cell sorting (FACS). BM-MSCs were purchased from ATCC (ATCC, Manassas, VA, USA).

2.2. Immunophenotyping

Flow cytometry was used to determine cell surface marker profile. Briefly, the cells were grown to 70% confluency, tryspinized, washed with PBS and pelleted. Cells (10^6) were stained with FITC labelled antibodies, CD34, CD44, CD45, and CD90 or APC labelled antibodies, CD29, CD73, and CD105 (Becton Dickinson) and then analysed on a FACS Canto II (Becton Dickinson) using Diva Software (Beckton Dickinson).

2.3. Differentiation of UC-MSCs into chondroprogenitor cells

UC-MSCs were induced towards chondrogenic lineage by culturing them in medium containing 20 ng TGFβ1, 10 ng insulin, 100 nM dexamethasone and 100 μM ascorbic acid. Following 2 weeks of culture, differentiated cells, CPCs were characterized by alcian blue 8GX (Sigma) and immunocytochemical staining as well as FACS and quantitative reverse transcriptase polymerase chain reaction (qRT-PCR) analysis for the expression of specific markers.

DOI: 10.1002/term

2.4. Alcian blue staining

Cells were fixed in 4% paraformaldehyde (USB Products, Cleveland, OH, USA) for 10 min at room temperature. After fixation, they were washed with PBS and stained with 1% alcian Blue solution (Sigma) in the dark for 1 h at room temperature, washed three times with PBS and visualized under a light microscope. Blue staining indicated synthesis of proteoglycans by chondrocytes.

2.5. Immunocytochemical analysis

Cells were fixed with 4% paraformaldehyde for 10 min at room temperature. They were then permeabilized with 0.5% Triton X-100 (Sigma) and blocked in 2% bovine serum albumin (Sigma) in PBS for 1 h and subjected to primary antibody at 1:100 dilutions at 4°C overnight followed by incubation with secondary antibody at 1:200 dilutions at 37°C for 1 h. Fluorescently labelled samples were counterstained with DAPI at 1:200 dilutions for 5 min at room temperature. Fluorescent images were captured using a confocal microscope (NIKON Instruments Inc, Melville, NY, USA). The primary and secondary antibodies used are listed in Table 1.

2.6. Experimental animals

All animal experiments were approved by the Animal Care Committee (ACC), Beaumont Health Systems, Royal Oak, Michigan (ACC#AL-13-06) and Institutional Biosafety Committee (IBC), Oakland University, Rochester, Michigan (IBC#2858). A total of 27 skeletally mature female New Zealand white rabbits, aged 6–12 months, weighing between 3.2 and 3.5 kg, were used. An initial MRI analysis was performed following the procedure described below on all rabbits under sedation to confirm that no previous disc degeneration was present, particularly either in the control (L3-4) or experimental (L2-3) or punctured (L4-5) IVDs.

2.7. Percutaneous induction intervertebral disc degeneration

Degeneration of IVD was induced following a previously published protocol (Sheikh *et al*., 2009). Briefly, each rabbit was initially tranquilized by intramuscular injection of xylazine (5 mg/kg) and ketamine (35 mg/kg), and buprenorphine 0.03 mg/kg and then placed on supplemental oxygen supplied through a face mask. The hairs were shaved from the lumbar sacroiliac portion of the mid-back of the animal. After induction of general anaesthesia, the field was prepped with betadine, and draped in a sterile, surgical fashion. A mini fluoroscopic unit was then used to identify the levels in the lumbar spine. A lateral approach from the rabbit's right flank was taken to enter the disc segment of interest. A 16-gauge needle was then advanced into the disc space through the Kambin's triangle, starting approximately 3 cm off the midline at the level of interest. To guide needle placement, anteroposterior (AP) and lateral fluoroscopic imaging were used. The needle was advanced until fluoroscopic confirmation showed the needle tip to be in the centre of the disc. Needle punctures of the IVDs on L2-3 and L4-5 were performed and L3-4 was left as undegenerated control. Following the procedure, rabbits were returned to their respective cages.

Table 1. List of primary and secondary antibodies used in immunohistochemical staining

Antibody	Primary	Secondary
SOX9	Rabbit polyclonal	Anti-rabbit-FITC
ACAN	Rabbit polyclonal	Anti-rabbit-FITC
COL2	Goat polyclonal	Anti-goat-FITC
FOXF1	Goat polyclonal	Anti-goat-FITC
TUBB	Goat polyclonal	Anti-goat-FITC

2.8. Evaluation of intervertebral discs using MRI

Each rabbit was initially tranquilized by intramuscular injection of xylazine (5 mg/kg) and ketamine (35 mg/kg) and then placed supine within the MRI imager coil (General Electric Medical Systems, Waukesha, WI, USA). A localizing mid-sagittal T2-weighted image was obtained to view the L2-3 to L4-5 intervertebral levels. Next, 3 mm thick mid sagittal sections were taken using T2-weighted imaging sequences to evaluate signal characteristics within the IVD. The MRI evaluations were performed initially on healthy rabbits as stated above and 2 weeks after the disc injury.

2.9. Fluorochrome labelling and transplantation of cells into degenerated rabbit IVD model

Cells were labelled with long-term cell membrane labelling dye PKH26 (Sigma) following the instructions of the supplier. Briefly, cells were washed with DMEM without FBS and collected as a loose pellet by centrifugation at 400 ***g*** for 5 min. The pellet was re-suspended in Diluent C and quickly mixed with the dye solution. The cell/dye suspension was then incubated at 37°C for 5 min, after which the reaction was stopped by adding an equal volume of FBS. Viability of the cells was measured by staining with trypan blue. Flow cytometry and confocal microscopy were used to confirm efficiency of fluorescent labelling of the cells prior to transplantation.

Following 2 weeks of degeneration, rabbits were anesthetized and prepared for the surgical procedure. The animals were injected with 20 μl of DMEM containing PKH26 labelled UC-10^6 MSCs ($n = 3$), 10^6 CPCs ($n = 3$) or medium alone (sham, $n = 3$) through a 22-gauge needle, using a 25-μl Hamilton syringe under the guidance of AP and lateral fluoroscopy. In all animals, one IVD, L3-4, and one IVD, L4-5 served as healthy and punctured control, respectively. The above experiment was performed

in triplicates. The animals were followed up to 8 weeks after the cell transplantation.

2.10. Tracking of transplanted cells and histological analysis

Post-treatment IVDs were harvested from the lumbar region of the rabbit spine with the help of a surgical bone saw after 8 weeks of transplantation. The intact IVDs were fixed in 4% paraformaldehyde overnight and then decalcified using 11% formic acid overnight in a beaker with continuous stirring. The IVDs were cleaned with scalpel by scraping the remaining excess bone on both sides. IVDs were then transferred into 30% sucrose overnight at room temperature and then embedded in OCT medium. Sections (6–10 μm thick) were prepared longitudinally. The sections were observed under confocal microscopy for the presence of PKH26 dye (Cy3), through which the transplanted cells were tracked if they were in the site of injection/implantation.

The sections were stained with haematoxylin and eosin (H&E) to evaluate the cellular architecture. The sections were also stained with periodic acid–Schiff (PAS) to detect sulfated proteoglycan distribution and alcian blue to estimate the extracellular matrix and were counterstained with nuclear fast red to visualize the presence of cells. To detect the protein levels of NP specific marker distributions in the repair tissue, the specimen section slides were incubated in primary antibodies SOX9, ACAN, collagen 2 (COL2), FOXF1 and β-tubulin (TUBB), followed by respective secondary antibodies listed in Table 1. Nonimmune rabbit immunoglobulin was used as negative control. Histological analysis of the repair tissue was performed by three individual observers blinded to the sample origin.

2.11. NP content and sulfated glycosaminoglycan analysis

Post-treatment IVDs were harvested after 8 weeks of transplantation; NP and AF were extracted separately. NP wet weight was measured and the changes were expressed as percentages. Percentages were calculated by the ratio of wet weight of the experimental IVD over wet weight of control IVD and multiplied by 100. Proteins were extracted by digesting the tissues with 125 μg/ml papain (Sigma) in 100 mM sodium phosphate buffer containing 10 mM EDTA, pH 6.5 at 55°C for 16 h. Tissue lysates were vortexed multiple times and cleared by centrifugation. sGAGs were determined by incubating the lysate with dimethylmethylene blue dye in glycine/NaCl solution, pH 3.0 and the complex formed was quantified spectrophotometrically at absorbance 525 nm. Total sGAG content was determined by using the chondroitin sulfate as a standard and was normalized to the dry weights of the samples. Analysis was performed in triplicate.

2.12. Analysis of IVD height

The MR images were analysed using Philips DICOM viewer version R3.0 SP3 (Philips Healthcare Company, Briarcliff Manor, NY, USA). The heights of the IVDs were measured at each level L2-3, L3-4 and L4-5. The measurements were taken by three individual blinded observers. IVD heights were determined from the average of the three measured values – measured at the centre of the disc space between the upper and lower vertebral bodies in the sagittal T2-weighted MRI images at the L2-3, L3-4 and L4-5.

2.13. qRT-PCR analysis

Total cellular mRNA was isolated using the Gene JET RNA purification Kit (Thermo Scientific), following the manufacturer's instructions. Total RNA was purified by incubation with DNase at 37°C for 30 min by using a thermocycler (Bio-Rad, Hercules, CA, USA). cDNA was synthesized by using BioRad iScript kit (Bio-Rad). qRT-PCR was performed by using Sso-Advanced Universal SYBR Green Supermix Kit (Bio-Rad) on CFX96 Real-Time System (Bio-Rad). A 10-μl reaction was used including 5 μl of Syber green, 3 μl of distilled H_2O, 0.5 μl of forward primer, 0.5 μl of reverse primer and 1 μl of 1:10 diluted cDNA. Each reaction was subjected to the following conditions: 98°C for 10 min, followed by 44 cycles of 98°C for 30 s, 60°C for 20 s, and 72°C for 30 s in 96-well optical reaction plates (Bio-Rad). Reference genes, GAPDH and ACTIN, were used to normalize the amplification of the target genes. Each qRT-PCR analysis was performed in triplicate. Primer sequences are listed in Table 2.

2.14. Statistical analysis

Data are presented as the mean ± standard error of the mean (SEM) of triplicates per analysis. Results with $*p \leq 0.05$, $**p \leq 0.01$ were considered statistically significant. All analyses were performed using SPSS version 11.5 (SPSS Inc. USA) using one-way ANOVA test.

3. Results

3.1. Isolation, characterization and differentiation of UC-MSCs into CPCs

Briefly, UC-MSCs were isolated from UC by explant culturing which showed fibroblastoid morphology (Figure 1A), expressed MSC specific markers (Figure 1B and C). To compare the therapeutic potential of UC-MSCs with their chondrogenic derivatives, UC-MSCs were induced to differentiate by culturing them in chondrogenic medium for 2 weeks. Unlike UC-MSCs, the differentiated cells displayed large flat morphology (Figure 1A). Molecular analysis showed that MSC surface markers, CD29, CD44, CD73, CD90 and CD105, were downregulated in about 50% of the chondrogenic derivatives (Figure 1B and C)

Table 2. List of primer sequences used in qRT-PCR

Gene	Primer sequence		
	Forward (5′–3 ′)	Reverse (5′–3′)	Product Length
hSOX9	AGCGAACGCACATCAAGAC	CTGTAGGCGATCTGTTGGGG	85
hACAN	AGCCTGCGCTCCAATGACT	GGAACACGATGCCTTTCACC	103
hCOL2	CTCGTGGCAGAGATGGAGAA	CACCAGGTTCACCAGGATTG	252
hFOXF1	AAGCCGCCCTATTCCTACATC	GCGCTTGGTGGGTGAACT	63
hKRT19	GCCACTACTACACGACCATCC	CAAACTTGGTTCGGAAGTCAT	126
hTGFβ1	GACACCAACTATTGCTTCAG	CAGGCTCCAAATGTAGGG	156
hTGFβ3	CGCCTCAAGAAGCAGAAG	TGTCGGAAGTCAATGTAGAG	182
hVCAN	GTCTCCTCCTCGGCTCTG	ACCTAATGTTCTCGGCTGTTG	141
hGDF5	ATCAGCATCCTCTTCATTGACTCT	ACACGACTCCACGACCAT	75
hGDF10	TGCCTAAGATCGTTCGTCCAT	CCCAAGGGAGTTCATCTTATCG	119
hGAPDH	ACAACTTTGGTATCGTGGAAGG	GCCATCACGCCACAGTTTC	101
hACTIN	AATCTGGCACCACACCTTCTAC	ATAGCACAGCCTGGATAGCAAC	170
rSOX9	TACGACTGGACGCTGGTGC	CGGGTGGTCTTTCTTGTGCT	261
rACAN	GAGGATGGCTTCCACCAGT	TGGGGTACCTGACAGTCTGA	61
rCOL2	ACAGCAGGTTCACCTATACCG	CCCACTTACCGGTGTGTTTC	60
rRUNX2	CAGGCAGTTCCCAAGCATTTCA	TGGTGGCAGGTAGGTATGGTAGT	154
rGAPDH	ACTTTGTGAAGCTCATTTCCTGGTA	GTGGTTTGAGGGCTCTTACTCCTT	107
rACTIN	CCCATCTACGAGGGCTACGC	TCCTTGATGTCCCGCACGATC	152

with concomitant upregulation of chondrogenic genes, such as SOX9, ACAN, COL2, TGFβ1, TGFβ3, VCAN and GDF10 (Figure 1D). Furthermore, these cells expressed chondroprogenitors specific proteins SOX9, ACAN, COL2, and FOXF1 (Figure 1E) suggesting that UC-MSCs differentiated into CPCs. Comparative analysis with BM-MSCs indicated that UC-MSCs had greater colony forming efficiency and proliferation capacity (Figure S1A). BM-MSCs population doubling time was significantly higher and increased rapidly upon successive passages. BM-MSCs stopped proliferating after P7 (Figure S1B). Furthermore, UC-MSCs exhibited higher chondrogenic differentiation compared to BM-MSCs as evidenced from the intensity of toluidine blue staining of the pellet sections (Figure S1C).

3.2. Degeneration of rabbit intervertebral discs and transplantation of UC-MSC and CPCs

To develop the rabbit model of DDD, IVDs were degenerated by using a needle puncture as previously described (Sheikh *et al*., 2009). Two weeks after puncturing IVDs, MRI analysis showed that punctured IVDs, L2-3 and L4-5 display degeneration of NP (Figure 2A). To determine changes at molecular levels in the NP of IVDs, transcription of specific genes involved in the maintenance of normal physiological function of IVDs were analysed by qRT-PCR. The results showed approximately 50% down-regulation of SOX9, ACAN, COL2 and RUNX, which further confirmed the degeneration of NP of the punctured IVDs (Figure 2B). The degenerated IVDs were then used for transplantation studies. To track the transplanted cells, they were labelled with PKH26 and trypan blue staining indicated that labelling did not affect the cell viability (Figure 2C). The efficiency of cell labelling assessed by flow cytometry was determined to be 97% and 96% for UC-MSCs and CPCs, respectively (Figure 2D). Labelled cells were then injected into the degenerated L2-3 IVDs, under the guidance of the c-arm fluoroscopy (Figure 2 E). A representative needle path for IVD puncture, cells or medium injections performed using Kambin's triangle approach is depicted in the Figure S2. AP and lateral image recordings helped proper placement of cells into the IVDs. The animals transplanted with labelled cells were followed for 8 weeks prior to scarification of animals and extraction of spine for IVDs analyses.

3.3. Physicochemical and histological evaluation of IVDs transplanted with UC-MSCs and CPCs

To investigate the effect of transplanted cells, the physicochemical properties of the NP of extracted IVDs were analysed. NP content of punctured and sham IVDs were reduced ~50% by weight. NP of the sham IVDs was similar or slightly more degenerated than the punctured IVDs, which might be due to the second intervention, medium injection. In punctured IVDs recipient of UC-MSCs and CPCs, the NP content increased by 16% and 33%, respectively (Figure 3A and B). Further analyses of NP showed significant increase in water and sGAG contents in CPCs and UC-MSCs treated IVDs (Figure 3C and D). Evidently, injection CPCs had more pronounced effect than UC-MSCs and they restored these components of the NP to near control. The height of punctured/sham IVDs was increased in response to transplantation of UC-MSCs and CPCs. However, IVD height was more significantly increased in the case of CPCs treated IVDs (Figure 3E).

Analysis of NP in punctured IVDs using H&E staining showed ossification of NP region, decreased cellularity, possibly due to the loss of extracellular matrix content as evident from the shrunken morphology with some fissuring appearance in the NP region, and the loss of fibrous connection in the AF region. However, NP of IVDs transplanted with UC-MSCs and CPCs appeared to have a cellular pattern different than NP of punctured IVDs. Particularly in the case of CPCs treated IVDs, cellular patterns resembled to that of chondromas in the NP of control IVDs. In fact, the cells appeared larger in IVDs injected with human CPCs, suggesting that xenogeneic cells survived, integrated and were distinct from the host cells. UC-MSCs treated IVDs showed only slight

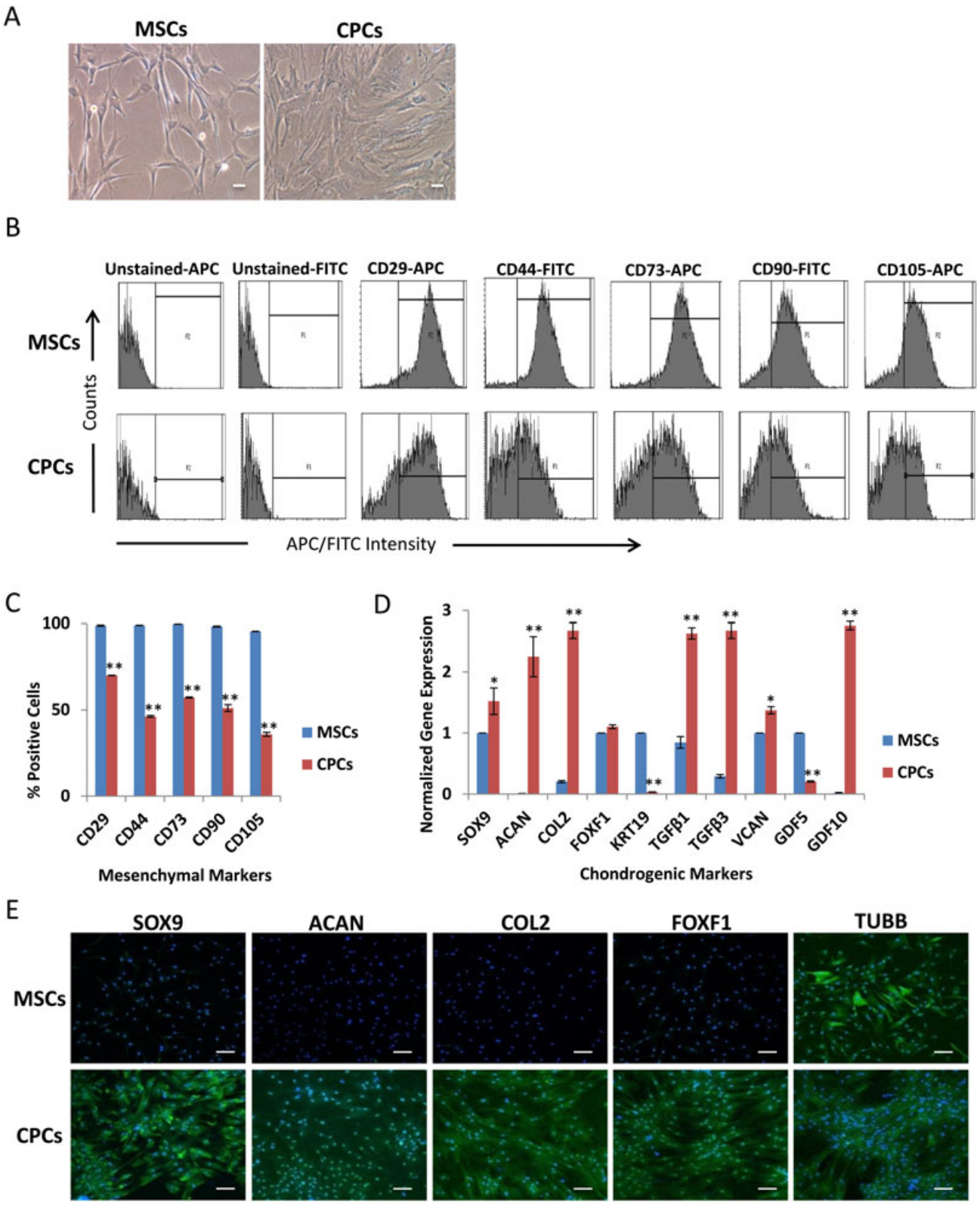

Figure 1. Characterization of CPCs derived from human UC-MSCs. (A) Phase contrast image of the UC-MSCs and CPCs derived from UC-MSCs. (B and C) Histograms and graphical representation of expression of mesenchymal markers in UC-MSCs and CPCs as determined by flow cytometry. All experiments were carried out in triplicate. (D) Expression of chondrogenic markers in CPCs as determined by qRT-PCR. Gene expression was normalized to GAPDH and actin and error bars represent the SEM of triplicate experiments. (E) Expression of chondrogenic proteins in CPCs as visualized by immunocytostaining using antibodies against SOX9, ACAN, COL2, FOXF1 and TUBB. Shown are merge images of DAPI (blue) and human antibodies (green). All scale bars represent 100 μm (Magnification: 10×)

improvement in the cellularity of NP (Figure 4A). Likewise, PAS and alcian blue staining of NP also indicated a significant increase in sGAG, glycoprotein contents of ECM, and cellular distribution as evident by the nuclear fast red counterstain in both CPCs and UC-MSCs transplanted IVDs (Figure 4B and C). However, increases in the water, sGAG, and NP contents as well as IVD height were more robust in case of CPCs treated IVDs suggesting that CPCs displayed higher potential to regenerate NP.

DOI: 10.1002/term

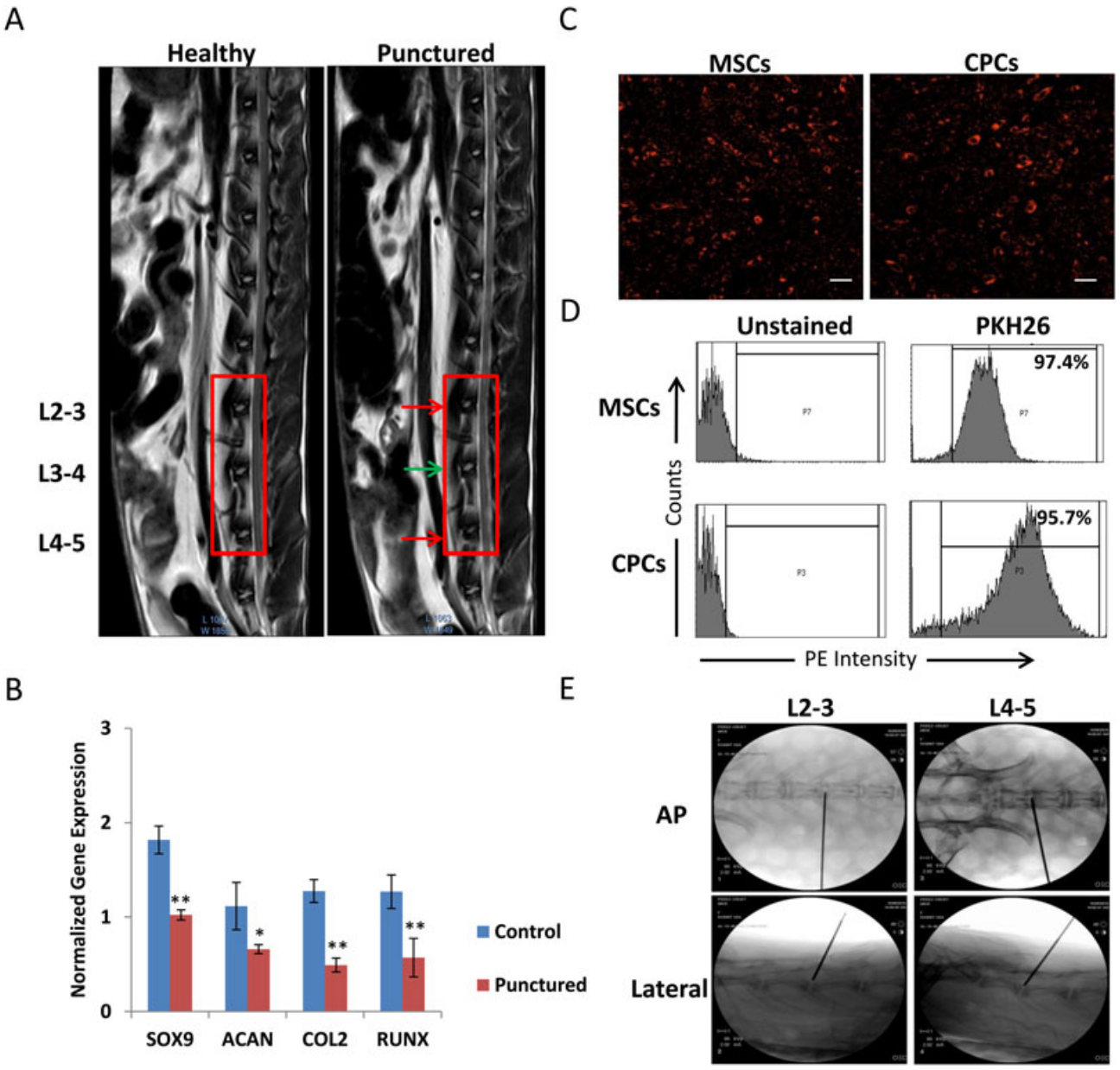

Figure 2. Analysis of degenerated rabbit IVDs, PKH26 labelled human cells and transplantation method. (A) Healthy vs. punctured IVDs of lumbar spines. Sagittal T2-weighted MRI images, showing the L2-3, L3-4 and L4-5 IVDs. Red and green arrows show the punctured and the punctured and control IVDs, respectively. (B) Expression of rabbit chondrogenic genes, SOX9, ACAN, COL2 and RUNX, in IVDs determined by qRT-PCR. Gene expression was normalized to GAPDH and ACTIN and error bars represent the SEM of the triplicate experiments. (C) Confocal images of the labelled UC-MSCs and CPCs. Scale bars represent 100 μm (magnification: 4×). (D) Flow cytometric analysis of labelled UC-MSCs and CPCs. (E) Fluoroscopic images of rabbit lumbar spine and Hamilton syringe needle used for injection of cells into IVDs

3.4. Xenogeneic expression of human chondrogenic and NP specific markers

Based on the physicochemical and histological evidence, it can be concluded that UC-MSCs and CPCs improved the structural integrity of IVDs although to a variable degree. To confirm whether the transplanted cells were functionally active, transcription and translation analyses of human NP specific markers were performed. Transcription analysis showed that chondrogenic and NP specific human genes, ACAN, COL2, FOXF1 and KRT19, were expressed at higher levels in CPCs than UC-MSCs transplanted IVDs. Higher expression of SOX9 in UC-MSCs *in vivo* could be attributed to their more differentiated state towards chondrogenic lineage (Figure 5A). The fact that chondrogenic specific human genes, particularly ACAN and COL2, were expressed higher *in vivo* (IVDs treated with UC-MSCs) than *in vitro*, suggest that xenogeneic microenvironment promoted differentiation of UC-MSCs towards chondrogenic lineage. Translational analysis confirmed the expression of chondrogenic and NP specific human proteins, SOX9, ACAN, COL2 and FOXF1 in the transplanted IVDs. Expectedly, the expression of these proteins was significantly higher in CPCs than UC-MSCs transplanted IVDs. Immunohistochemical analysis also showed colocalized expression of these proteins with a housekeeping protein TUBB as well as cell labelling dye, PKH26 (Figure 5B). The

DOI: 10.1002/term

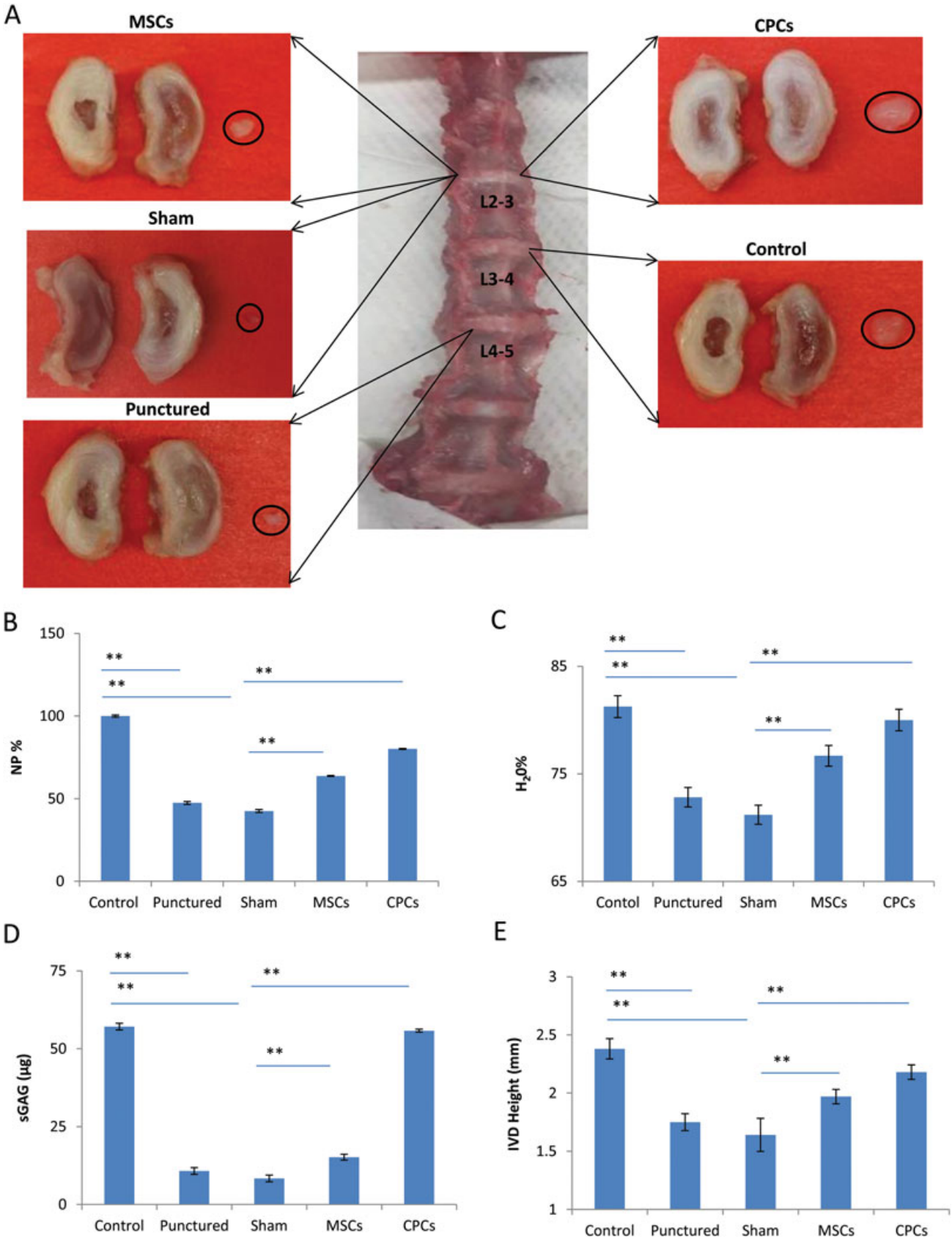

Figure 3. Physicochemical analysis of rabbit IVDs transplanted with human cells. (A) Spine, extracted 8 weeks post-treatment, displaying control IVD (L3-4), treated IVDs (L2-3) with UC-MSCs or CPCs or medium alone (sham) and punctured IVDs (L4-5) and their respective NP content. (B–E) Bar graphs representing control, punctured, sham, and treated IVDs with UC-MSCs or CPCs, analysed for NP, water, sGAG and height, respectively

transplanted labelled cells dispersed into the damaged/degenerated areas of IVDs. As expected, the control, punctured and sham IVDs did not show presence of labelled cells or expression of human markers. Again,

DOI: 10.1002/term

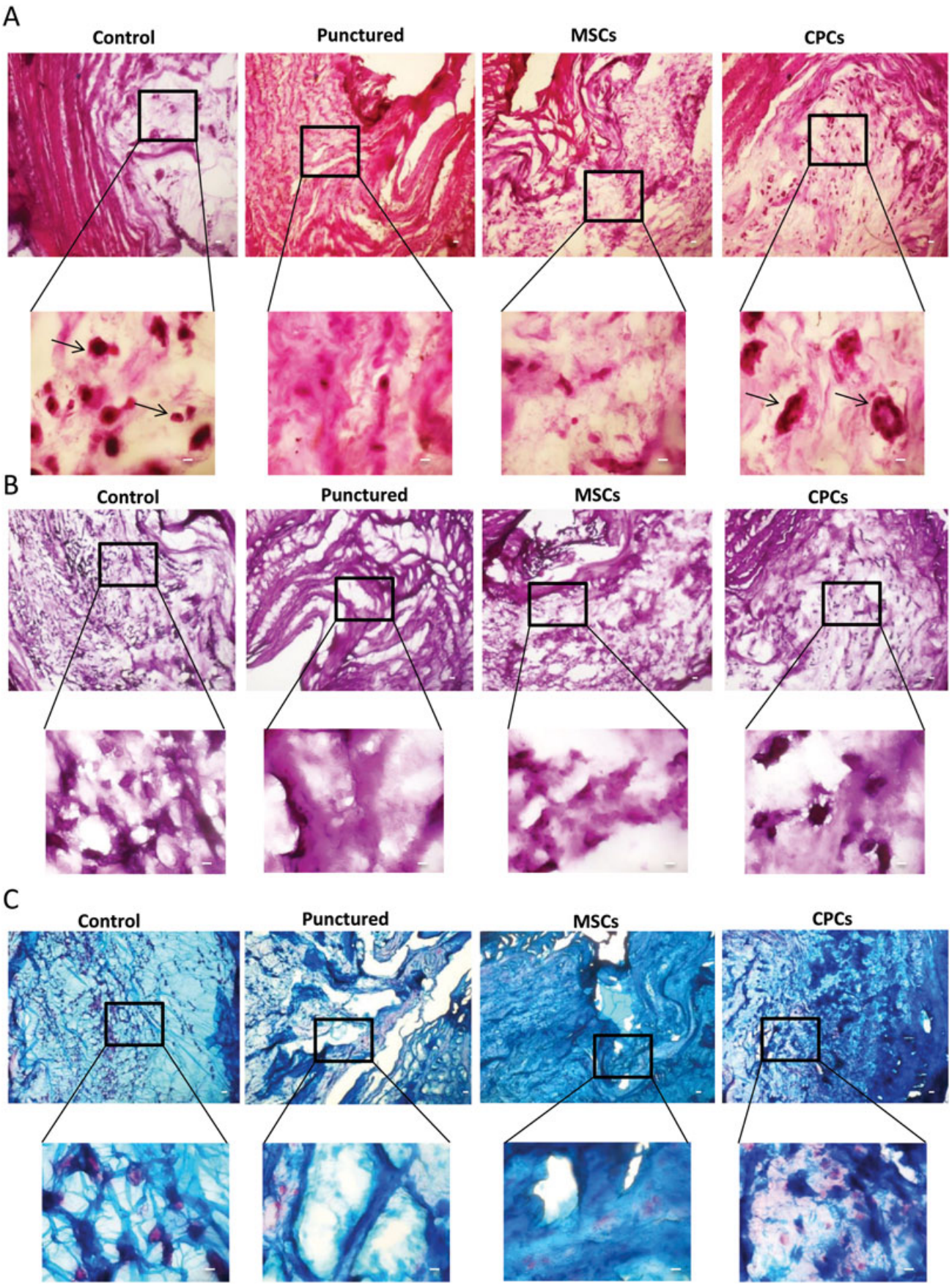

Figure 4. Histological analysis of rabbit IVDs transplanted with human cells. (A–C) Histological analysis of the NP stained with H&E, PAS and alcian blue displaying intracellular morphology, presence of glycoproteins, and the extracellular matrix proteins, respectively. All scale bars represent 100 μm (magnification: 4×) and inserts represent 100 μm (magnification: 40×)

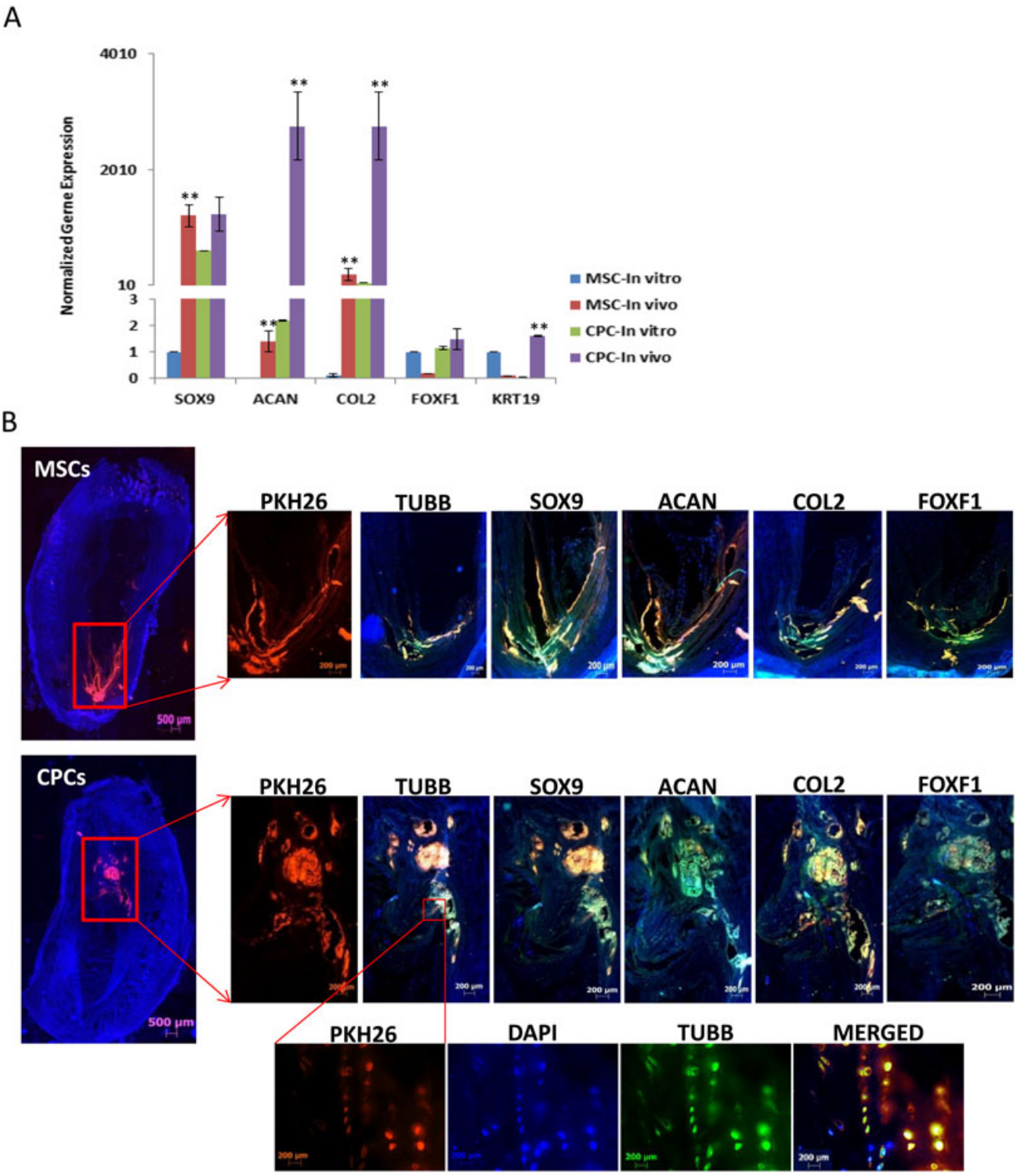

Figure 5. Expression of chondrogenic and NP specific human markers in transplanted IVDs. (A) Expression of SOX9, ACAN, COL2, FOXF1 and KRT19 in UC-MSCs and CPCs used for injection (*in vitro*) and transplanted IVDs (*in vivo*) as determined by qRT-PCR. Gene expression was normalized to GAPDH and ACTIN and error bars represent the SEM of triplicate experiments. (B) Histochemical analysis of IVDs transplanted with labelled UC-MSCs and CPCs. Red, blue and green represent the cell labelling dye PKH26, DAPI staining the nuclei, and antibodies labelling human proteins (TUBB, SOX9, ACAN, COL2 and FOXF1), respectively. The displayed inserts (top two rows) are high magnification (200 µm) merged images of PKH26, DAPI, and labelled antibodies as determined by confocal microscopy. Bottom row represents high magnification (200 µm) of TUBB inserts showing individual channel of PKH26, DAPI and TUBB antibody and merged image. Scale bars represent 500 µm (Magnification: 5×) and inserts represent 200 µm (Magnification: 20×). Insert of TUBB represents 200 µm (Magnification: 40×)

translation of these markers was significantly higher in CPCs than UC-MSCs transplanted IVDs. It is important to note that expression of human specific markers, SOX9, ACAN, COL2 and FOXF1 as well as TUBB was also observed in AF of the IVDs, which was localized with the PKH dye signal. It can be speculated that the transplanted cells were either not fully placed into the NP during injection or they were leaked out from NP of the IVDs or both. Collectively, these results suggest that the transplanted cells survived, integrated and dispersed as well as were

DOI: 10.1002/term

functionally active, into both the inner AF and the NP of IVDs.

4. Discussion

Human degenerative diseases such as DDD inflict huge economic burden costing billions of dollars in healthcare. Stem cell therapy is considered to have the potential to treat such debilitating diseases. Although direct evidence for regeneration has been limited, a few studies showed matrix synthesis or expression of ACAN, SOX9 and COL2 attributed to structural improvement of IVD following the transplantation of human adult MSCs (Chun *et al*., 2012; Henriksson *et al*., 2009; Jeong *et al*., 2010; Marfia *et al*., 2014; Sakai *et al*., 2003). One of the reasons for the paucity of such studies with adult MSCs could be due to the fact that isolation of MSCs from adult sources requires invasive procedures and yields poor cell recovery (Bentivegna *et al*., 2013; Liu *et al*., 2013). Moreover, differentiation of MSCs and characterization of their chondrogenic derivatives as well as use for subsequent transplantation studies require higher quantities of MSCs than is currently feasible. These limitations in the quantity and quality of adult MSCs have prompted investigations to search for alternative sources of cells for therapeutic applications.

The alternative studies led to isolation of MSCs from perinatal sources, which are more primitive, potent and proliferative, and can be acceptable for allogeneic and xenogeneic transplantation studies (Beeravolu *et al*., 2016; Rachakatla *et al*., 2007; Weiss and Troyer, 2006). Consequently, several reports have indicated that perinatal MSCs have the potential to produce ECM which is an integral component of NP of the IVD (Anderson *et al*., 2013; Chon *et al*., 2013; Ibrahim *et al*., 2015; Li *et al*., 2015, 2016).

We hypothesized that perinatal stem cells, such as UC-MSCs and their derivatives, can survive in the avascular NP environment with long-term viability to regenerate damaged IVD in a rabbit model for DDD. In this study, tracking of labelled human cells showed survival, dispersed and integration of UC-MSCs and CPCs in the damaged IVDs. An increase in NP content in the IVDs transplanted with human cells provided preliminary evidence of regeneration of the NP. Importantly, the effect of CPCs on NP content was more pronounced than UC-MSCs. The analysis of the physicochemical composition of NP retrieved from the transplanted IVDs indicated increase in water and sGAG content in both UC-MSCs and CPCs. However, only CPCs transplanted IVDs showed higher water and sGAG contents at levels comparable to healthy IVDs. Although studies have used MRI analysis to measure NP intensities (Henriksson *et al*., 2009; Jeong *et al*., 2010; Marfia *et al*., 2014; Zhang *et al*., 2015) and estimate water content (Ahn *et al*., 2015), the restoration of physicochemical properties of the NP using human cells has not been reported in *in vivo* studies. The broader aspects of NP regeneration and metabolic activity of the IVD, such as nutrient exchange and shock absorbance capacity, would be manifested by restoration of sGAG, NP and water contents in the ECM (Erwin and Hood, 2014).

Another measure to assess IVDs is the histological analysis showing ECM content and presence of cellularity, proteoglycans and glycoproteins. Our results indicated a substantial improvement in the histology and cellularity as well as ECM regeneration as evident from the increase in glycoproteins and proteoglycan content of the transplanted IVDs, particularly with CPCs. In addition, PAS staining also displayed an increase in the amount and distribution of sGAG in the transplanted IVDs. Similar to our results on UC-MSCs, a few studies have shown improvement in the cellularity and ECM production by the transplantation of human BM and adipose MSCs using only histological evidences (Chun *et al*., 2012; Henriksson *et al*., 2009; Jeong *et al*., 2010; Marfia *et al*., 2014), while no *in vivo* study has indicated improvement in the quantification of sGAG content upon transplantation of human cells.

The xenogeneic nature of the transplanted cells allowed us to selectively evaluate the human specific chondrogenic and NP markers that could contribute to regenerate NP. Results showed that three human chondrogenic markers, SOX9, ACAN and COL2, were upregulated at both transcriptional and translational levels in the IVDs transplanted with human cells. Furthermore, these proteins were coexpressed with the human specific TUBB suggesting that the expression of these proteins was from transplanted cells. Since, the exact cell types present in the NP is debatable and markers which exclusively identify NP cells are not known, particularly in human IVDs, presence of chondrogenic markers alone does not necessarily implicate the differentiation of MSCs into NP lineage. This prompted us to further evaluation of transcription and translation of FOXF1 and KRT19, which have been putatively used as human NP specific markers (Han *et al*., 2015; Rodrigues-Pinto *et al*., 2013). No other study has investigated NP marker expression upon transplantation of human cells in DDD animal models.

Not unexpectedly, the expression of human chondrogenic and NP specific genes was highly upregulated in IVDs recipient of CPCs. In the case of UC-MSCs, a limited increase in chondrogenic and decrease in NP markers was observed. This suggests that the signaling cues from the IVD microenvironment played a role in modulating the expression of NP specific human genes more effectively in CPCs than in UC-MSCs. It is also important to consider that cytokines secreted by MSCs injected into the degenerated IVD could activate endogenous cells to induce their migration and the production of other paracrine signals, which could contribute to repair and regeneration (Krock *et al*., 2015; Yim *et al*., 2014). Furthermore, it has been suggested that NP cells and matrix components in IVD have positive modulatory effects on transplanted MSCs to differentiate them towards an NP-like phenotype *in vivo* (Krock *et al*., 2015). However, evidence to support that MSCs transplanted in

DOI: 10.1002/term

the IVDs can differentiate into NP cells is lacking because the outcomes are more difficult to interpret due to a lack of well-defined NP vs. chondrocyte markers (Krock *et al*., 2015; Yim *et al*., 2014). Therefore, evidence of NP regeneration is generally based on the collective outcomes of physicochemical, histological, molecular and MRI analysis.

While the overall results of this study suggest the efficacy and potential of human UC-MSCs and CPCs for regeneration of NP, the effect of transplanted cells on the host's molecular, cellular and structural regeneration capacity were not studied in this investigation. MSCs are not known to be involved in the generation of NP *in vivo*; therefore, it can be speculated that MSCs transplanted directly into IVD may not be as potent as their chondrogenic derivatives. Nonetheless, for the first time, this study compared the regenerative potential of human UC-MSCs and CPCs, and showed that CPCs could be more effective in repairing or regenerating damaged tissue. Further studies are warranted to the explore the mechanism involved in regenerating the NP by UC-MSCs and CPCs *in vivo*.

Also, importantly human cells transplanted into rabbit IVDs did not elicit immune response. MSCs have been reported to be largely safe for IVD regeneration in xenograft models (Hee *et al*., 2010; Wei *et al*., 2009; Yim *et al*., 2014). Previous reports indicate a lack of immune response using *in vivo* human MSC xenograft models, suggesting that IVD is an immune-privileged site (Sheikh *et al*., 2009; Wei *et al*., 2009). In addition, perinatal MSCs do not require tissue matching and have lower risk of graft-vs.-host disease; therefore, any donor can give MSCs to any person without rejection or need for immunosuppressive agents (Weiss *et al*., 2008).

In conclusion, this study demonstrated that human UC-MSCs are a promising cell source but their differentiation into CPCs prior to transplantation can be more efficacious for the treatment of DDD. Results from this study should also provide basis to explore wider therapeutic use of human UC-MSCs.

Acknowledgements

The study was supported by OU-WB ISCRM, Oakland University and Michigan Head and Spine Institute. N. Beeravolu received Provost Graduate Research Award from Oakland University for this project. I. Khan was supported by Dr Panjwani Center for Molecular Medicine and Drug Research, Pakistan. The authors acknowledge Dr S. Chintala, Eye Research Institute for help with confocal microscopy. We also thank E. Morrison, M. McGonagle, and H. Brzezinski for help in animal studies as well as Dr Y. Seonghwan and J. Wloch for MRI. We are very thankful to Dr C. Govind, Dr L. Villa, and Dr M. Craig for reviewing the manuscript.

Conflict of interest

The authors have declared that there is no conflict of interest.

References

Ahn J, Park EM, Kim BJ *et al*. 2015; Transplantation of human Wharton's jelly-derived mesenchymal stem cells highly expressing TGFβ receptors in a rabbit model of disc degeneration. *Stem Cell Res Ther* **6**: 190.

Alghamdi S, Khan I, Beeravolu N *et al*. 2016; BET protein inhibitor JQ1 inhibits growth and modulates WNT signaling in mesenchymal stem cells. *Stem Cell Res Ther* **7**: 22.

Amini AR, Laurencin CT, Nukavarapu SP. 2012; Bone tissue engineering: recent advances and challenges. *Crit Rev Biomed Eng* **40**(5): 363–408.

Anderson DG, Markova D, An HS *et al*. 2013; Human umbilical cord blood-derived mesenchymal stem cells in the cultured rabbit intervertebral disc: a novel cell source for disc repair. *Am J Phys Med Rehabil* **92**: 420–429.

Arufe MC, De la Fuente A, Fuentes I *et al*. 2011; Umbilical cord as a mesenchymal stem cell source for treating joint pathologies. *World J Orthop* **2**: 43–50.

Beeravolu N, Khan I, McKee C *et al*. 2016; Isolation and comparative analysis of potential stem/progenitor cells from different regions of human umbilical cord. *Stem Cell Res* **16**: 696–711.

Bentivegna A, Miloso M, Riva G *et al*. 2013; DNA methylation changes during *in vitro* propagation of human mesenchymal stem cells: implications for their genomic stability? *Stem Cells Int* **2013**: 192425.

Bian Z, Sun J. 2015; Development of a KLD-12 polypeptide/TGF-β1-tissue scaffold promoting the differentiation of mesenchymal stem cell into nucleus pulposus-like cells for treatment of intervertebral disc degeneration. *Int J Clin Exp Pathol* **8**: 1093–1103.

Chon BH, Lee BJ, Jing L *et al*. 2013; Human umbilical cord mesenchymal stromal cells exhibit immature nucleus pulposus cell phenotype in a laminin-rich pseudo-three-dimensional culture system. *Stem Cell Res Ther* **4**(5): 120.

Chun HJ, Kim YS, Kim BK *et al*. 2012; Transplantation of human adipose-derived stem cells in a rabbit model of traumatic degeneration of lumbar discs. *World Neurosurg* **78**: 364–371.

Ciapetti G, Granchi D, Devescovi V *et al*. 2012; *Ex vivo* observation of human intervertebral disc tissue and cells isolated from degenerated intervertebral discs. *Eur Spine J* **21**: S10–S19.

Clarke LE, McConnell JC, Sherratt MJ *et al*. 2014; Growth differentiation factor 6 and transforming growth factor-beta differentially mediate mesenchymal stem cell differentiation, composition, and micromechanical properties of nucleus pulposus constructs. *Arthritis Res Ther* **16**(2): R67. http://doi.org/10.1186/ar4505

Clouet J, Pot-Vaucel M, Grimandi G *et al*. 2011; Characterization of the age-dependent intervertebral disc changes in rabbit by correlation between MRI, histology and gene expression. *BMC Musculoskelet Disord* **12**: 147.

Colombier P, Clouet J, Boyer C *et al*. 2016; TGF-beta1 and GDF5 act synergistically to drive the differentiation of human adipose stromal cells toward nucleus pulposus-like cells. *Stem Cells* **34**: 653–667.

Erwin WM, Hood KE. 2014; The cellular and molecular biology of the intervertebral disc: A clinician's primer. *J Can Chiropr Assoc* **58**: 246–257.

Espinoza N, Peterson M. 2012; How to depolarise the ethical debate over human embryonic stem cell research (and other ethical debates too!). *J Med Ethics* **38**: 496–500.

Gupta MS, Cooper ES, Nicoll SB. 2011; Transforming growth factor-beta 3 stimulates cartilage matrix elaboration by human marrow-derived stromal cells encapsulated in photocrosslinked carboxymethylcellulose hydrogels: potential for nucleus pulposus replacement. *Tissue Eng Part A* **17**: 2903–2910.

Han XB, Zhang YL, Li HY *et al*. 2015; Differentiation of human ligamentum flavum stem cells toward nucleus pulposus-like cells induced by coculture system and hypoxia. *Spine (Phila Pa 1976)* **40**: E665–E674.

Hee HT, Ismail HD, Lim CT *et al*. 2010; Effects of implantation of bone marrow mesenchymal stem cells, disc distraction and combined therapy on reversing degeneration of the intervertebral disc. *J Bone Joint Surg Br* **92**: 726–736.

Henriksson HB, Svanvik T, Jonsson M *et al*. 2009; Transplantation of human mesenchymal stems cells into intervertebral discs in a xenogeneic porcine model. *Spine* **34**: 141–148.

Hua J, Qiu P, Zhu H *et al*. 2011; Multipotent mesenchymal stem cells (MSCs) from human umbilical cord: potential differentiation of germ cells. *Afr J Biochem Res* **5**: 113–123.

Ibrahim AM, Elgharabawi NM, Makhlouf MM *et al*. 2015; Chondrogenic differentiation of human umbilical cord blood-derived mesenchymal stem cells *in vitro*. *Microsc Res Tech* **78**: 667–675.

Jeong JH, Lee JH, Jin ES *et al*. 2010; Regeneration of intervertebral discs in a rat disc degeneration model by implanted adipose-tissue-derived stromal cells. *Acta Neurochir* **152**: 1771–1777.

Kim KW, Lim TH, Kim JG *et al*. 2003; The origin of chondrocytes in the nucleus pulposus and histologic findings associated with the transition of a notochordal nucleus pulposus. *Spine* **28**(10): 982–990.

Korecki CL, Taboas JM, Tuan RS *et al*. 2010; Notochordal cell conditioned medium stimulates mesenchymal stem cell differentiation toward a young nucleus pulposus phenotype. *Stem Cell Res Ther* **1**: 18.

Krock E, Rosenzweig DH, Haglund L. 2015; The inflammatory milieu of the degenerate disc: is mesenchymal stem cell-based therapy for intervertebral disc repair a feasible approach? *Curr Stem Cell Res Ther* **10**: 317–328.

Leckie SK, Sowa GA, Bechara BP *et al*. 2013; Injection of human umbilical tissue-derived cells into the nucleus pulposus alters the course of intervertebral disc degeneration *in vivo*. *Spine J* **13**: 263–272.
Li X, Chang H, Luo H *et al*. 2015; Poly (3-hydroxybutyrate-co-3-hydroxyhexanoate) scaffolds coated with PhaP-RGD fusion protein promotes the proliferation and chondrogenic differentiation of human umbilical cord mesenchymal stem cells in *vitro*. *J Biomed Mater Res A* **103**: 1169–1175.
Li X, Duan L, Liang Y *et al*. 2016; Human umbilical cord blood-derived mesenchymal stem cells contribute to chondrogenesis in coculture with chondrocytes. *Biomed Res Int* **2016**: 3827057.
Liu L, Cheung TH, Charville GW *et al*. 2013; Chromatin modifications as determinants of muscle stem cell quiescence and chronological aging. *Cell Rep* **4**: 189–204.
Lo B, Parham L. 2009; Ethical issues in stem cell research. *Endocr Rev* **30**: 204–213.
Marfia G, Campanella R, Navone SE *et al*. 2014; Potential use of human adipose mesenchymal stromal cells for intervertebral disc regeneration. *Arthritis Res Ther* **16**: 457.
Nouh MR. 2012; Spinal fusion-hardware construct: basic concepts and imaging review. *World J Radiol* **4**: 193–207.
Pang X, Yang H, Peng B. 2014; Human umbilical cord mesenchymal stem cell transplantation for the treatment of chronic discogenic low back pain. *Pain Physician* **17**(4): E525–E530.
Pera MF. 2001; Scientific considerations relating to the ethics of the use of human embryonic stem cells in research and medicine. *Reprod Fertil Dev* **13**: 23–29.
Pfleger ADWB. 2003; Burden of major musculoskeletal conditions. *Bull World Health Organ* **81**(9): 646–656.
Purmessur D, Schek M, Abbott RD *et al*. 2011; Notochordal conditioned media from tissue increases proteoglycan accumulation and promotes a healthy nucleus pulposus phenotype in human mesenchymal stem cells. *Arthritis Res Ther* **13**(3): R81.
Rachakatla RS, Marini F, Weiss ML *et al*. 2007; Development of human umbilical cord matrix stem cell-based gene therapy for experimental lung tumors. *Cancer Gene Ther* **14**: 828–835.
Rodrigues-Pinto R, Richardson SM, Hoyland JA. 2013; Identification of novel nucleus pulposus markers. *Bone Joint Res* **2**: 169–178.
Sakai D, Mochida J, Yamamoto Y *et al*. 2003; Transplantation of mesenchymal stem cells embedded in Atelocollagen® gel to the intervertebral disc: a potential therapeutic model for disc degeneration. *Biomaterials* **24**: 3531–3541.
Sheikh H, Zakharian K, De La Torre RP *et al*. 2009; *In vivo* intervertebral disc regeneration using stem cell-derived chondroprogenitors. *J Neurosurg Spine* **10**: 265–272.
Shim EK, Lee JS, Kim DE *et al*. 2016; Autogenous mesenchymal stem cells from the vertebral body enhance intervertebral disc regeneration by paracrine interaction: an *in vitro* pilot study. *Cell Transplant* [Epub ahead of print].
Song K, Gu T, Shuang F *et al*. 2015; Adipose-derived stem cells improve the viability of nucleus pulposus cells in degenerated intervertebral discs. *Mol Med Rep* **12**: 4664–4668.
Strassburg S, Richardson SM, Freemont AJ *et al*. 2010; Co-culture induces mesenchymal stem cell differentiation and modulation of the degenerate human nucleus pulposus cell phenotype. *Regen Med* **5**(5): 701–711.
Teschendorff AE, Jones A, Fiegl H *et al*. 2012; Epigenetic variability in cells of normal cytology is associated with the risk of future morphological transformation. *Genome Med* **4**: 24.
Wei A, Tao H, Chung SA *et al*. 2009; The fate of transplanted xenogeneic bone marrow-derived stem cells in rat intervertebral discs. *J Orthop Res* **27**: 374–379.
Weiss ML, Anderson C, Medicetty S *et al*. 2008; Immune properties of human umbilical cord Wharton's jelly-derived cells. *Stem Cells* **26**: 2865–2874.
Weiss ML, Troyer DL. 2006; Stem cells in the umbilical cord. *Stem Cell Rev* **2**: 155–162.
Yim RL, Lee JT, Bow CH *et al*. 2014; A systematic review of the safety and efficacy of mesenchymal stem cells for disc degeneration: insights and future directions for regenerative therapeutics. *Stem Cells Dev* **23**; 2553–2567.
Zhang Y, Tao H, Gu T *et al*. 2015; The effects of human Wharton's jelly cell transplantation on the intervertebral disc in a canine disc degeneration model. *Stem Cell Res Ther* **6**: 154.

Supporting information

Additional Supporting Information may be found online in the supporting information tab for this article.

Figure S1. Comparison of BM and UC derived MSCs. (A) Colony forming efficiency, (B) Population doublings, and (C) Differentiation into chondroprogenitor cells as determined by Toluidine blue staining after three weeks of pellet culturing in chondrogenic differentiation medium. UC-MSC pellet grew significantly larger size and stained more intensely than BM-MSC pellet.
Figure S2. Macroscopic images of the IVDs showing the site of puncture or injection of cells. (A and B) cryosections of control and punctured IVDs, respectively and (C) longitudinal cut opened view of whole IVD transplanted with the cells. Arrows indicate the path of the needle used for puncturing and injecting the cells using the Kambin's triangle approach.